DALTON
FULL PAPER

Coordination behaviour of (diaryl disulfide)-bridged dinuclear thiairidaindan cores: ligand substitution by isocyanides, CO, hydrazines and hydroxylamine, and related reactions †

Shoji Matsukawa,[a] Shigeki Kuwata,‡[a] Youichi Ishii *§[a] and Masanobu Hidai *[b]

[a] *Department of Chemistry and Biotechnology, Graduate School of Engineering, The University of Tokyo, Hongo, Bunkyo-ku, Tokyo 113-8656, Japan*
[b] *Department of Materials Science and Technology, Faculty of Industrial Science and Technology, Science University of Tokyo, Noda, Chiba 278-8510, Japan*

Received 12th February 2002, Accepted 15th May 2002
First published as an Advance Article on the web 5th June 2002

The diaryl disulfide ligand in the thiolato-bridged diiridium(III) complexes [{Ir(μ-$SC_6H_{4-n}Me_nCH_2$)Cl(PPh_3)}$_2$(μ-ArSSAr)] [**1a**, n = 1, Ar = $C_6H_3Me_2$-2,6 (Xy); **1b**, n = 2, Ar = $C_6H_2Me_3$-2,4,6 (Mes)] is readily substituted by isocyanides, CO, hydroxylamine and hydrazines to afford the bis(isocyanide), bis(carbonyl) and bis(hydroxylamine) complexes [Ir(μ-$SC_6H_{4-n}Me_nCH_2$)Cl(PPh_3)(L)]$_2$ (**2a**, n = 1, L = XyNC; **2b**, n = 2, L = XyNC; **3a**, n = 1, L = Bu^{t}NC; **3b**, n = 2, L = Bu^{t}NC; **4a**, n = 1, L = CO; **4b**, n = 2, L = CO; **7a**, n = 1, L = NH_2OH; **7b**, n = 2, L = NH_2OH) and the bridging hydrazine complexes [{Ir(μ-$SC_6H_{4-n}Me_nCH_2$)Cl(PPh_3)}$_2$(μ-NH_2NR_2)] (**5a**, n = 1, R = H; **5b**, n = 2, R = H; **6**, n = 1, R = Me), respectively. On the other hand, the reaction of **1b** with MeLi resulted in reductive cleavage of the disulfide bond to give the coordinatively unsaturated diiridium(III) complex [Ir(μ-$SC_6H_2Me_2CH_2$)(SMes)(PPh_3)]$_2$ (**8**), which was further converted into the bis(carbonyl) complex [Ir(μ-$SC_6H_2Me_2CH_2$)(SMes)(PPh_3)(CO)]$_2$ (**9**) upon addition of CO. Treatment of **2b** with $AgPF_6$ led to the formation of the difluorophosphato-bridged complex [{Ir(μ-$SC_6H_2Me_2CH_2$)(PPh_3)(XyNC)}$_2$(μ-PF_2O_2)][PF_6] (**10**). The structures of the thiairidaindan complexes **2b**, **4a**, **5a**, **7a** and **8**–**10** have been determined by X-ray crystallography.

Introduction

Coordination of substrates onto multimetallic centres is the first and a fundamental step in activation and transformation of these substrates on polynuclear complexes, a subject which has received much attention in relation to catalysis involving metal surfaces and metalloenzymes.[1] In the course of our studies on nitrosyl–thiolato complexes,[2,3] we have recently prepared the dinuclear thiairidaindan complexes [{Ir(μ-$SC_6H_{4-n}Me_nCH_2$)Cl(PPh_3)}$_2$(μ-ArSSAr)] [**1a**, n = 1, Ar = $C_6H_3Me_2$-2,6 (Xy); **1b**, n = 2, Ar = $C_6H_2Me_3$-2,4,6 (Mes)] through the reaction of Ir(I) nitrosyl–bis(arenethiolato) complexes with PhCOCl, which involves the activation of a benzyl C–H bond, the oxidative coupling of the arenethiolato ligand and the unexpected substitution of the nitrosyl ligand by a chloride anion (eqn. 1).[3] Complexes **1** also feature a bridging organodisulfide ligand, the chemistry of which remains undeveloped.[4] We envisaged that liberation of the diaryl disulfide ligand in **1** would lead to the formation of a doubly coordinatively unsaturated platform suitable for the bimetallic activation and transformation of substrates, because the thiairidaindan framework is expected to offer rigid and highly directional vacant sites in close proximity without fragmentation of the dinuclear core. Within this context, and in relation to our continuing studies on thiolato-bridged dinuclear complexes of noble metals,[5] we describe here the substitution of the bridging diaryl disulfide ligand in **1** by a wide range of substrates, including π-acceptor (CO, isocyanides) and σ-donor (hydrazines) ligands, both of which are known to be substrates or inhibitors of nitrogenase, a typical metalloenzyme with a sulfur-bridged multimetallic core.[6]

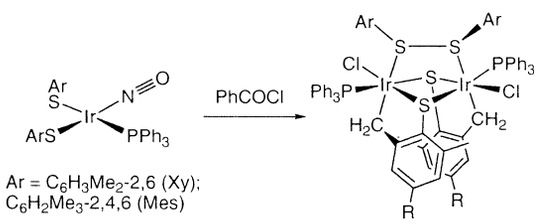

Ar = $C_6H_3Me_2$-2,6 (Xy); $C_6H_2Me_3$-2,4,6 (Mes)

1a, R = H, Ar = Xy; **1b**, R = Me, Ar = Mes

(1)

Results and discussion

Reaction of 1 with isocyanides

The diaryl disulfide ligand in **1** was smoothly replaced by 2,6-xylyl isocyanide to afford the diiridium(III) bis(isocyanide) complexes [Ir(μ-$SC_6H_{4-n}Me_nCH_2$)Cl(PPh_3)(XyNC)]$_2$ (**2a**, n = 1; **2b**, n = 2) in good yield (Scheme 1). The detailed structure of **2** has been unambiguously determined by an X-ray diffraction study using a single crystal of **2b** (Fig. 1). The important interatomic distances and bond angles are listed in Table 1. The molecule has a crystallographically imposed C_2 axis bisecting the Ir–Ir vector. Like the parent complexes **1**, complex **2b** has a *syn*-dimeric thiairidaindan framework connected through the sulfur atoms. It is of interest that, because of this rigid

† Electronic supplementary information (ESI) available: selected interatomic distances and angles for **4a**·0.5$C_6H_5CH_3$ (Table S1) and **9**·2CH_2Cl_2 (Table S2). See http://www.rsc.org/suppdata/dt/b2/b201591a/

‡ Present address: Department of Applied Chemistry, Graduate School of Science and Engineering, Tokyo Institute of Technology, O-okayama, Meguro-ku, Tokyo 152-8552, Japan.

§ Present address: Department of Applied Chemistry, Faculty of Science and Engineering, Chuo University, Kasuga, Bunkyo-ku, Tokyo 112-8551, Japan.

DOI: 10.1039/b201591a

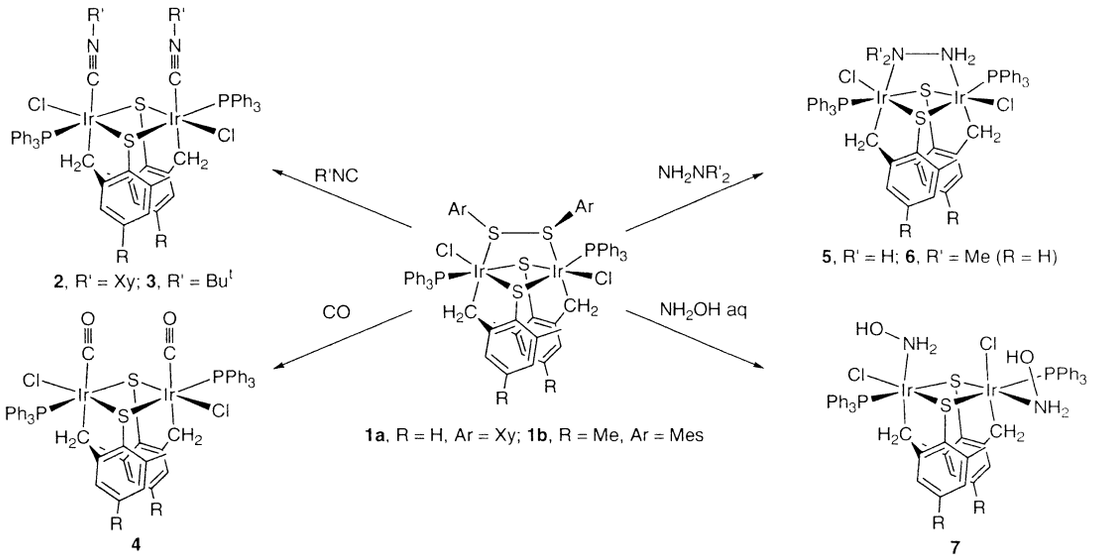

Scheme 1

Table 1 Selected interatomic distances (Å) and bond angles (°) in **2b**[a]

Ir(1)–Ir(1*)	3.605(1)	C(28)–N(1)	1.149(8)
Ir(1)–S(1)	2.323(1)	C(28)–C(28*)	3.469(11)
Ir(1)–S(1*)	2.465(1)	N(1)–N(1*)	3.423(9)
Ir(1)–P(1)	2.323(2)	C(29)–C(29*)	3.55(2)
Ir(1)–Cl(1)	2.410(2)	Ir(1)–C(28)–N(1)	179.2(6)
Ir(1)–C(7)	2.097(6)	C(28)–N(1)–C(29)	169.9(8)
Ir(1)–C(28)	1.987(6)		

[a] Starred atoms have been generated by a symmetry operation ($-x$, y, $1/2 - z$).

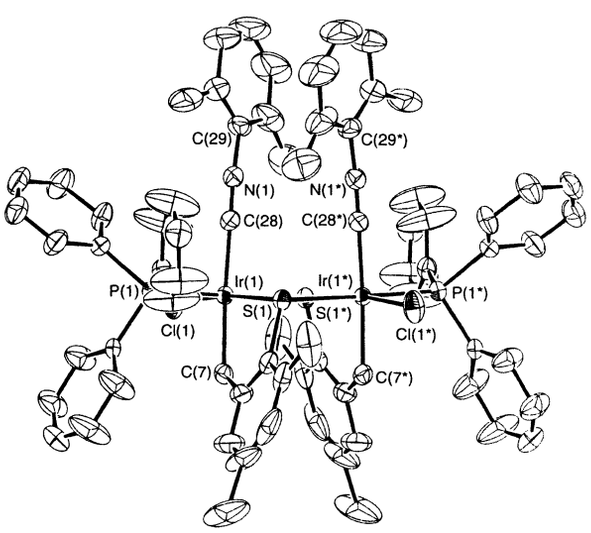

Fig. 1 Molecular structure of **2b**. All hydrogen atoms are omitted for clarity.

framework, the two mutually *cis*-oriented isocyanide ligands are almost parallel to each other in close proximity: the C(28)–C(28*), N(1)–N(1*) and C(29)–C(29*) distances are 3.469(11), 3.423(9) and 3.55(2) Å, respectively. The Ir_2S_2 face in **2b** is almost planar, with a dihedral angle of 5.4° around the S–S

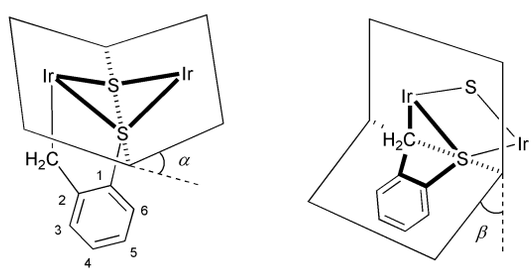

Fig. 2 Definition of the dihedral angles in the Ir_2S_2 planes (α) and thiairidacycles (β). Position numbers in the thiairidaindan skeleton for assignment of the ^{1}H NMR signals (see Table 7) are also indicated.

vector, in contrast with the puckered Ir_2S_2 face in **1b** (Table 2, Fig. 2). This flattening, probably due to the absence of a third bridging ligand on the Ir_2S_2 face, causes another structural difference between the triply bridged complex **1b** and the doubly bridged complex **2b**. Namely, the thiairidaindan skeletons are almost planar in **1b**, whereas those in **2b** are folded by about 20° along the S–C(methylene) vectors to retain the tetrahedral geometry around the sulfur atoms (Table 2, Fig. 2). The Ir–Ir distance of 3.605(1) Å precludes any metal–metal bonding.

In accordance with the solid state structure, the ^{31}P-{^{1}H} NMR spectra of **2** reveal only one singlet, attributed to the PPh_3 ligands, and the ^{1}H NMR spectra show that the two thiairidaindan parts, as well as the two isocyanide ligands, are equivalent. Only one of the two mutually coupled doublets for the diastereotopic methylene protons in the thiairidacycle is split by the phosphorous nucleus. Given that the ^3J(PH) values are sensitive to the P–Ir–C–H dihedral angles for these protons, this observation suggests that the octahedral configuration of the Ir atom and, consequently, the dinuclear structure of **2** are maintained, even in solution. On the other hand, the *ortho*-methyl groups in the isocyanide ligands give only a broad signal at room temperature. This signal changes into one sharp singlet at 50 °C, whereas it is resolved into two sharp singlets at −80 °C. Obviously, this temperature-dependent behaviour is due to the sterically restricted rotation around the Ir–C–N–C axes that lie

Table 2 Dihedral angles between planes in the Ir_2S_2 faces (α) and thiairidacycles (β)[a]

	1b	**2b**	**4a**·0.5$C_6H_5CH_3$	**5a**·Pr^{i}OH	**7a**·Et_2O	**8**·0.5CH_2Cl_2	**9**·2CH_2Cl_2	**10**·CH_2Cl_2
α/°	27.1	5.4	3.5	32.8	15.4	33.2	17.2	17.1
β/°	1.4, 5.6	20.4	20.6, 18.4	1.5, 0.6	7.8, 11.5	3.5, 3.7	12.6, 14.0	18.5, 11.3

[a] For the definition of the angles, see Fig. 2.

close to each other. The IR spectra of **2** exhibit only one NC stretching band around 2130 cm^{-1}.

The corresponding *tert*-butyl isocyanide complexes $[Ir(\mu\text{-}SC_6H_{4-n}Me_nCH_2)Cl(PPh_3)(Bu^tNC)]_2$ (**3a**, $n = 1$; **3b**, $n = 2$) were also obtained in a similar manner to complexes **2** (Scheme 1). The NMR and IR spectra, as well as a preliminary X-ray analysis of **3a**, have confirmed the dinuclear *syn*-bis(isocyanide) structure of **3**. In contrast to the xylyl isocyanide complexes **2**, no fluxional behaviour was observed in variable-temperature ^1H NMR measurements of **3**. It should be noted that the thiairidacycle in **2** and **3** is stable and insertion of the coordinated isocyanides into the Ir–CH_2 bonds did not take place.

Reaction of 1 with CO

The diaryl disulfide ligand in **1** was also replaced by a π-accepting ligand, CO, to afford the bis(carbonyl) complexes $[Ir(\mu\text{-}SC_6H_{4-n}Me_nCH_2)Cl(PPh_3)(CO)]_2$ (**4a**, $n = 1$; **4b**, $n = 2$) in essentially quantitative yield (Scheme 1). The IR spectra of **4** exhibit a strong CO stretching band around 2040 cm^{-1}, being comparable to those of Ir(III) carbonyl complexes such as $[IrCl_3(CO)(PPh_3)_2]$ (2080 cm^{-1})[7] and $[(C_5Me_5)IrCl(Ph)(CO)]$ (2025 cm^{-1}).[8] The NMR spectral features of **4** are in common with those of the related C_2-symmetrical complexes **1**–**3**. Furthermore, an X-ray analysis has elucidated the detailed structure of **4a** [Fig. 3 and Table S1 (ESI)]. The *syn*-dimeric thiairidaindan core structure of the carbonyl complex **4a** is quite similar to those of the isocyanide complexes **2** and **3**: the two carbonyl ligands lie *cis* to each other with respect to the almost planar Ir_2S_2 face and the thiairidacycles are folded toward outside of the molecule by about 20°. Like the isocyanide ligands in **2** and **3**, the carbonyl ligands did not insert into the Ir–CH_2 bonds under ambient conditions.

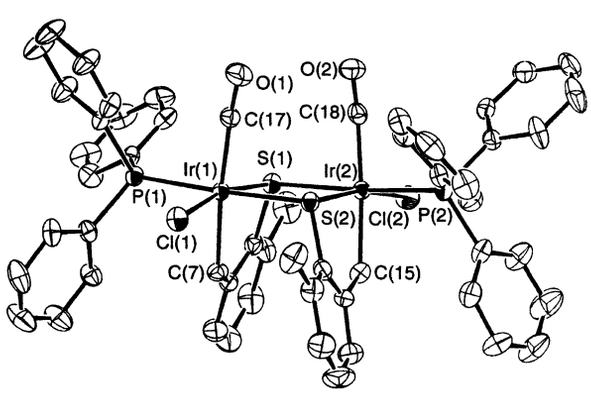

Fig. 3 Molecular structure of **4a**·0.5$C_6H_5CH_3$. Solvating $C_6H_5CH_3$ and all hydrogen atoms are omitted for clarity.

Reaction of 1 with hydrazines

Although a number of hydrazine complexes have been reported so far,[9] studies on sulfur-ligated di- or polynuclear complexes containing hydrazine ligands are still limited, despite their relevance to biological nitrogen fixation.[10] In connection with this, our group has previously reported the catalytic N–N bond cleavage of hydrazine on thiolato-bridged diruthenium complexes,[11] as well as the synthesis of $Mo_2Ir_2S_4$ cubane-type sulfido clusters having dialkylhydrazido(2−) ligands.[12] As an extension of these studies, we have investigated the reactivities of the thiairidacycle complexes **1** toward hydrazines.

When **1** was reacted with 1 equivalent of anhydrous hydrazine, the bridging mono(hydrazine) complexes $[\{IrCl(\mu\text{-}SC_6H_{4-n}Me_nCH_2)(PPh_3)\}_2(\mu\text{-}NH_2NH_2)]$ (**5a**, $n = 1$; **5b**, $n = 2$) were formed in good yield (Scheme 1). The crystal structure of **5a** is depicted in Fig. 4, whilst selected interatomic distances and angles are listed in Table 3. The hydrazine complexes **5** and the parent complexes **1** are closely related in structure,

Table 3 Selected interatomic distances (Å), bond angles (°) and torsion angles (°) in **5a**·Pr^iOH

Ir(1)–Ir(2)	3.376(1)	Ir(2)–N(2)	2.269(6)
Ir(1)–S(1)	2.280(2)	N(1)–N(2)	1.458(7)
Ir(1)–S(2)	2.423(2)	N(1)–O(1)	2.938(9)
Ir(2)–S(1)	2.439(2)	N(2)–O(1)	3.109(9)
Ir(2)–S(2)	2.285(2)	N–Ir–CH_2	168 (mean)
Ir–P	2.28 (mean)	Ir(1)–N(1)–N(2)	113.8(4)
Ir–Cl	2.42 (mean)	Ir(2)–N(2)–N(1)	112.2(4)
Ir–CH_2	2.07 (mean)	Ir(1)–N(1)–N(2)–Ir(2)	27.9(5)
Ir(1)–N(1)	2.253(6)		

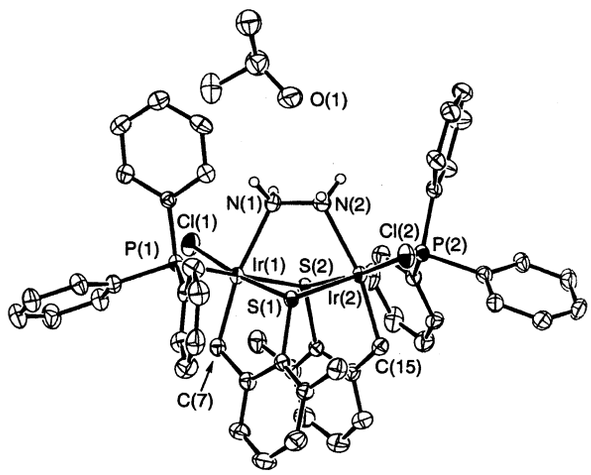

Fig. 4 Molecular structure of **5a**·Pr^iOH. All hydrogen atoms, except those in the bridging N_2H_4 ligand, are omitted for clarity.

except that the octahedral Ir(III) centres in **5** are bridged by a hydrazine molecule instead of the diaryl disulfide ligand. The bridging hydrazine ligand adopts a *cisoid* conformation, where the Ir–N–N–Ir dihedral angle is 27.9(5)°. The N–N bond distance of 1.458(7) Å is also unexceptional for a μ, η^1:η^1-hydrazine ligand,[9] whilst the Ir–N bond lengths of 2.26 Å (mean) are slightly longer than those found in iridium ammine complexes (2.067–2.15 Å).[13] The presence of NH ··· O hydrogen bonds between the coordinated hydrazine and the solvating 2-propanol molecule is indicated by the short N(1)–O(1) and N(2)–O(1) distances of 2.938(9) and 3.109(9) Å, respectively. It is worth pointing out that hydrazine complexes of iridium are very scarce,[14] and, to our knowledge, complex **5a** is the first example of an iridium hydrazine complex whose structure has been determined by X-ray crystallography.

In the ^1H NMR spectrum of **5a**, the chemically inequivalent geminal protons in the hydrazine ligand give rise to two doublets at δ 5.01 and 4.55 with a ^2J(HH) value of 6.3 Hz. Other spectral features, including those of the $^{31}P\text{-}\{^1H\}$ NMR spectrum, are also in agreement with the solid state structure of **5**.

We also attempted the reaction of **1** with 2 equivalents of hydrazine in order to prepare a bis(η^1-hydrazine) complex. However, the mono(hydrazine) complex **5** was the only product confirmed by $^{31}P\text{-}\{^1H\}$ NMR analysis of the reaction mixture.

Treatment of **1a** with *N*,*N*-dimethylhydrazine resulted in the formation of the bridging dimethylhydrazine complex $[\{IrCl(\mu\text{-}SC_6H_3MeCH_2)(PPh_3)\}_2(\mu\text{-}NH_2NMe_2)]$ (**6**). Although a single crystal of **6** was subjected to an X-ray diffraction study, the refinement of the structure of **6** could not be completed because of severe decay of the crystal during the data collection and disorder in the solvating molecule. Nevertheless, the preliminary analysis unambiguously confirmed the atom connection scheme of **6** and revealed significantly long Ir–NMe_2 distances (2.39 Å, mean of the two crystallographically independent molecules) compared to the Ir–NH_2 distances (2.20 Å, mean) as indicated in Fig. 5; the two Ir–N–N angles are also considerably different from each other. These structural

Table 4 Selected interatomic distances (Å) in **7a**·Et_2O

Ir(1)–Ir(2)	3.558(2)	Ir(2)–P(2)	2.301(1)
Ir(1)–Cl(1)	2.416(2)	Ir(1)–N(1)	2.232(5)
Ir(2)–Cl(2)	2.532(1)	Ir(2)–N(2)	2.127(4)
Ir(1)–S(1)	2.312(1)	Ir(1)–C(7)	2.079(5)
Ir(1)–S(2)	2.442(1)	Ir(2)–C(15)	2.071(5)
Ir(2)–S(1)	2.452(1)	Cl(1)–O(1)	3.039(5)
Ir(2)–S(2)	2.317(1)	Cl(2)–O(2)	3.007(6)
Ir(1)–P(1)	2.288(1)	N(1)–Cl(2)	3.131(5)

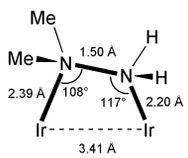

Fig. 5 Schematic representation of the bridging *N*,*N*-dimethylhydrazine ligand in **6**. All the indicated distances and angles are the averaged values of the two crystallographically independent molecules.

characteristics are in common with the related dimethylhydrazine complex [{(cod)RuH}{(cod)RuCl}(μ-H)(μ-Cl)(μ-NH_2NMe_2)] (cod = 1,5-cyclooctadiene),[15] a rare example of dialkylhydrazine-bridged complex, and can be explained by the steric effect of the methyl substituents on the nitrogen atom.

In accordance with the unsymmetrical structure of **6**, the ^{31}P-{^1H} NMR spectrum of **6** exhibits two doublets at δ −7.7 and −8.5 with a ^4J(PP) value of 15.1 Hz. The two methyl groups of the hydrazine ligands give rise to two singlets, indicating that the Ir–NMe_2 bond is preserved, even in solution, despite the long Ir–NMe_2 distance.

Reaction of 1 with hydroxylamine

Hydroxylamine, a molecule isoelectronic to hydrazine, has been the subject of much attention in the chemistry of inorganic nitrogen compounds[16] because it is invoked as a possible intermediate in the nitrate assimilation process, for example.[17] Indeed, hydroxylamine is one of the major products in the electrocatalytic reduction of nitrate anion at an iron porphyrin complex-modified electrode.[18] Nevertheless, studies on hydroxylamine complexes are surprisingly limited,[19] in contrast with those on hydrazine complexes, and polynuclear hydroxylamine complexes are unknown. To compare the reactivities of hydrazines and hydroxylamine, we next examined the reaction of **1** with hydroxylamine.

Treatment of **1** with 2 equivalents of hydroxylamine afforded the bis(hydroxylamine) complexes [Ir(μ-$SC_6H_{4-n}Me_nCH_2$)Cl(PPh$_3$)(NH_2OH)]$_2$ (**7a**, n = 1; **7b**, n = 2), as shown in Scheme 1. The hydroxylamine signals in the ^1H NMR spectra of **7** are subdivided into those for the two chemically inequivalent hydroxylamine ligands, distinguished by ^1H–^1H COSY measurements, although the NH and OH protons in each set of the signals have not been assigned. The ^{31}P-{^1H} NMR spectra of **7** exhibit two doublets with a ^4J(PP) value of 15.3 Hz, suggesting an unsymmetrical structure for **7**. An X-ray analysis of **7a** has been performed to clarify the detailed structure of **7**; the molecular structure is depicted in Fig. 6(a), whilst selected interatomic distances and angles are listed in Table 4. As in the bis(isocyanide) and bis(carbonyl) complexes **2**–**4**, one of the incoming hydroxylamine molecules is coordinated to the axial position of the Ir(1) atom with respect to the Ir_2S_2 face. In contrast, the other hydroxylamine on the Ir(2) atom lies in the equatorial plane and the axial position is occupied by a chloro ligand. This unsymmetrical coordination unique to the hydroxylamine complexes **7** can be explained by the stabilization effect of the intramolecular hydrogen bond network, as illustrated in Fig. 6(b). For example, the close O(1)–Cl(1) and H(61)–Cl(1) contacts [3.039(5) and 2.221 Å] as well as the O(1)–H(61)–Cl(1) angle (139.8°) indicate the presence of an OH ··· Cl hydrogen bond. A hydrogen bond interaction between the Cl(2) atom and

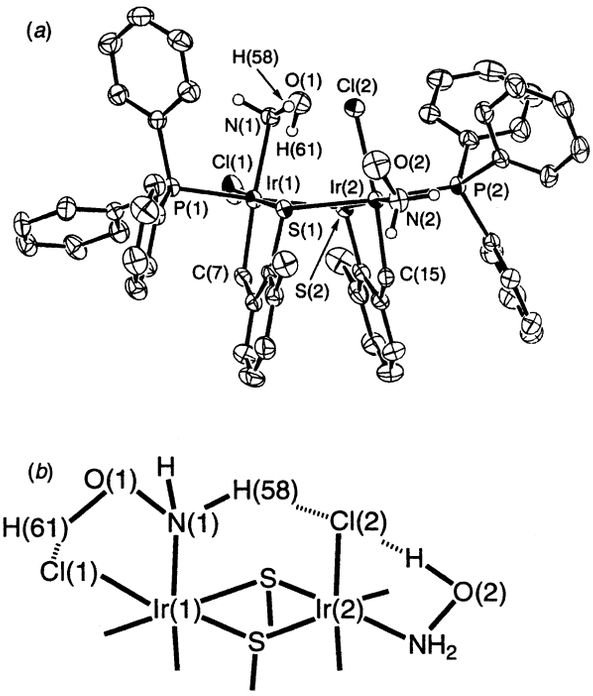

Fig. 6 (a) Molecular structure of **7a**·Et_2O and (b) schematic representation of the intramolecular hydrogen bond network in **7a**. Solvating Et_2O and all hydrogen atoms, except those of NH_2OH, are omitted in the molecular structure for clarity.

the hydroxylamine ligand on the Ir(2) atom is also suggested by the short O(2)–Cl(2) distance of 3.007(6) Å, although the hydroxy hydrogen atom bound to the O(2) atom could not be located in the X-ray analysis and, thus, the H–Cl distance is not available. In addition, an NH ··· Cl hydrogen bonding interaction is observed between the Cl(2) atom and the axial hydroxylamine ligand, with N(1)–Cl(2) and H(58)–Cl(2) distances of 3.131(5) and 2.244 Å, respectively; the N(1)–H(58)–Cl(2) angle is 155.0°. This NH ··· Cl hydrogen bonding leads to a slight folding of the Ir_2S_2 face, as in the triply bridged complexes **1** and **5**; the dihedral angle around the S–S vector is 15.4°. Apart from the relative positions of the hydroxylamine and chloro ligands, the whole structure of **7** is analogous to those of **1**–**6**. It should be noted that **7** represents a rare example of complexes having two or more hydroxylamine ligands.[19b]

The reaction of **1a** with an equimolar amount of hydroxylamine was also attempted in order to obtain a hydroxylamine-bridged complex related to the hydrazine-bridged complexes **5** and **6**. However, the reaction mixture was found to contain only **1a** and **7a** by ^{31}P-{^1H} NMR spectroscopy.

Reaction of 1b with MeLi

In view of the transformation of organic substrates at the diiridium core, we turned our attention to alkylation of **1** by replacing the chloro ligands. However, when **1b** was treated with 2 equivalents of MeLi, the thiolato complex [Ir(μ-$SC_6H_2Me_2CH_2$)(SMes)(PPh$_3$)]$_2$ (**8**) was obtained in moderate yield instead of the expected methyl complex (eqn. 2). In the present reaction, the diaryl disulfide ligand has formally been reduced by MeLi to the terminal thiolato ligands in **8**, although

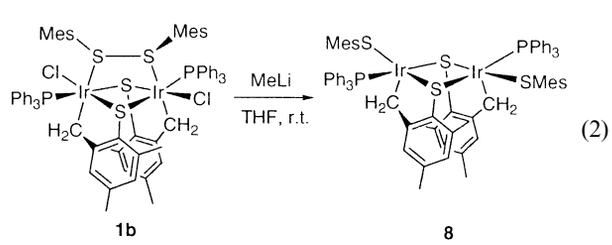

(2)

Table 5 Selected interatomic distances (Å) and bond angles (°) in **8**·0.5CH_2Cl_2

Ir(1)–Ir(2)	3.462(1)	P(1)–Ir(1)–S(2)	174.40(8)
Ir(1)–S(1)	2.353(2)	P(2)–Ir(2)–S(1)	172.92(9)
Ir(1)–S(2)	2.413(2)	S(1)–Ir(1)–S(3)	158.61(10)
Ir(1)–S(3)	2.296(3)	S(2)–Ir(2)–S(4)	157.37(9)
Ir(2)–S(1)	2.420(2)	S(1)–Ir(1)–C(7)	84.1(2)
Ir(2)–S(2)	2.339(2)	S(2)–Ir(2)–C(16)	84.1(2)
Ir(2)–S(4)	2.310(3)	S(3)–Ir(1)–C(7)	117.2(2)
Ir–P	2.295 (mean)	S(4)–Ir(2)–C(16)	118.4(3)
Ir–CH_2	2.08 (mean)	Ir–S–Mes	113 (mean)

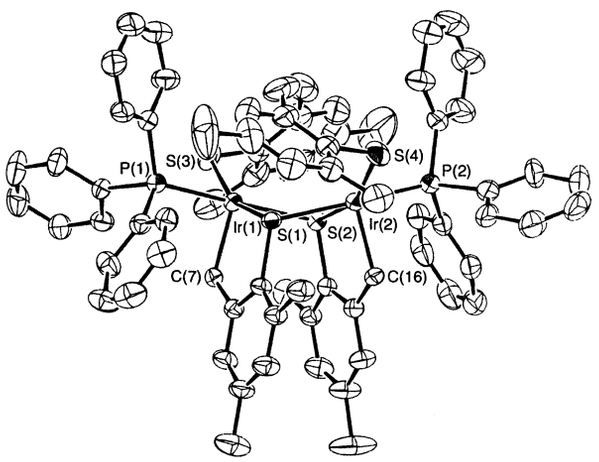

Fig. 7 Molecular structure of **8**·0.5CH_2Cl_2. Solvating CH_2Cl_2 and all hydrogen atoms are omitted for clarity.

we failed to detect ethane in the reaction mixture. An X-ray analysis has elucidated the molecular structure of **8**, which is depicted in Fig. 7; selected interatomic distances are listed in Table 5. The molecule has an approximate C_2 axis bisecting the Ir–Ir vector. Unlike the previously described complexes **1**–**7**, the Ir(III) centres in **8** adopt a distorted trigonal bipyramidal geometry. The equatorial plane contains the thiairidacycle and the terminal thiolato sulfur atom with a large S–Ir–S angle of 158° (mean). The phenyl groups of the terminal thiolato ligands are directed toward the open space *trans* to the methylene carbon atoms, although there is no evidence of agostic interactions between the mesityl groups in the thiolato ligands and the iridium centres. The Ir_2S_2 face is puckered, with an Ir–S–S–Ir dihedral angle of 33.2°. The Ir–Ir distance of 3.462(1) Å precludes any metal–metal bonding; consequently, the Ir(III) centres have only 16 electrons and are coordinatively unsaturated. Indeed, **8** is related to the species that would be generated by the liberation of the diaryl disulfide ligand from **1**. In spite of the coordinative unsaturation, the Ir–S distances in **8** are not so different from those in complexes **1**–**7**, suggesting that the π-donation of the lone pair electrons on the S atoms is not significant.

The ^{1}H NMR spectrum indicates the dynamic behaviour of **8** in solution. For example, the terminal thiolato ligands give rise to two broad signals for the 2- and 6-methyl groups at 20 °C, which are sharpened at lower temperatures and fused into one singlet at a coalescence temperature of 35 °C. In addition, the signals for the PPh_3 protons appear over the wide range δ 8.7–6.0 at 20 °C; they move to a range of δ 8.7–6.5 at −55 °C. These observations suggest that the rotation around the C–S bonds in the terminal thiolato ligands, as well as the Ir–P bonds, is strongly restricted by the steric congestion between these neighbouring ligands.

Reaction of 8 with CO

Taking account of the coordinative unsaturation of the Ir atoms in **8**, we examined the reaction of **8** with CO. The reaction proceeded smoothly to afford the 18-electron Ir(III) bis(carbonyl) complex [Ir(μ-$SC_6H_2Me_2CH_2$)(SMes)(PPh_3)(CO)]$_2$ (**9**) (eqn. 3). The detailed structure determined by an

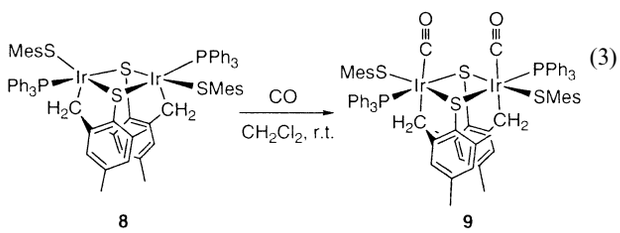

(3)

X-ray diffraction study is shown in Fig. 8, and the metrical parameters are collected in Table S2 (ESI). Complex **9** has a dinuclear thiairidaindan framework analogous to those of **1**–**7**, and the two CO ligands are bound on the Ir_2S_2 plane in a *syn* geometry, as in the closely related bis(carbonyl) complexes **4** having two chloro ligands instead of the two terminal thiolato ligands in **9**. The mesityl groups in the terminal thiolato ligands point up toward the CO ligands to avoid the steric congestion with the PPh_3 ligands and the thiairidacycles. The separation between the Ir atoms [3.649(1) Å] suggests the absence of any metal–metal interactions. The ν(CO) value of 2035 cm^{-1} in the IR spectrum of **9** is comparable to those for **4**.

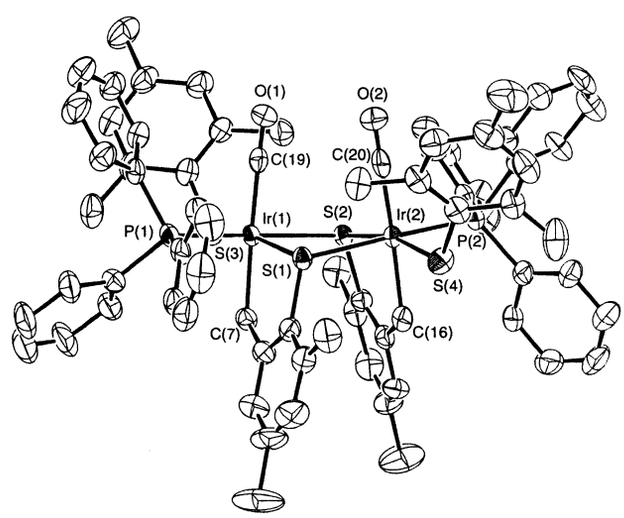

Fig. 8 Molecular structure of **9**·2CH_2Cl_2. Solvating CH_2Cl_2 and all hydrogen atoms are omitted for clarity.

The ^{1}H NMR spectrum of **9** is temperature-dependent, as is that of the parent complex **8**. The signals for the *ortho*-methyl and *meta*-aryl protons in the terminal thiolato ligands appear inequivalent at −60 °C, indicating that rotation around the C–S axes is slow at this temperature. At room temperature, these signals are greatly broadened, suggesting that the hindered rotation of the C–S bonds renders these protons equivalent.

On the other hand, the reaction of **8** with other substrates, such as *N*,*N*-dimethylhydrazine, gave a complex mixture of unidentified species. This is at least partly because the coordinatively unsaturated centres in **8** are much more crowded than those derived from **1**.

Reaction of 2 with $AgPF_6$

During our extensive studies on the reactivities of thiolato-bridged dinuclear chloro complexes having η^5-C_5Me_5 ligands,[5] we have already found that treatment of these complexes with silver cations is effective in producing open coordination sites on the dinuclear centres.[20] Thus, we carried out the reactions of the thiairidaindan complexes with silver cations to generate

Table 6 Selected interatomic distances (Å) and bond angles (°) in **10**·CH_2Cl_2

Ir(1)–Ir(2)	3.580(1)	P(3)–F	1.53 (mean)
Ir(1)–S(1)	2.376(2)	P(3)–O	1.46 (mean)
Ir(1)–S(2)	2.447(2)	IrC–NXy	1.16 (mean)
Ir(2)–S(1)	2.425(2)	Ir–C–N	174 (mean)
Ir(2)–S(2)	2.368(2)	IrC–N–C	171 (mean)
Ir–P	2.33 (mean)	O–Ir–CH_2	173 (mean)
Ir–CH_2	2.07 (mean)	F(1)–P(3)–F(2)	97.6(3)
Ir–CNXy	1.93 (mean)	O(1)–P(3)–O(2)	122.0(3)
Ir–O	2.28 (mean)		

vacant sites for further accumulation of substrates on the diiridium core.

The reaction of the bis(xylyl isocyanide) complex **2b** with 2 equivalents of $AgPF_6$ in dichloromethane resulted in the unexpected formation of the difluorophosphato-bridged complex [{Ir(μ-$SC_6H_2Me_2CH_2$)(PPh$_3$)(XyNC)}$_2$(μ-PF_2O_2)]-[PF_6] (**10**) (eqn. 4). The ^{31}P-{^{1}H} NMR spectrum of **10** exhibits

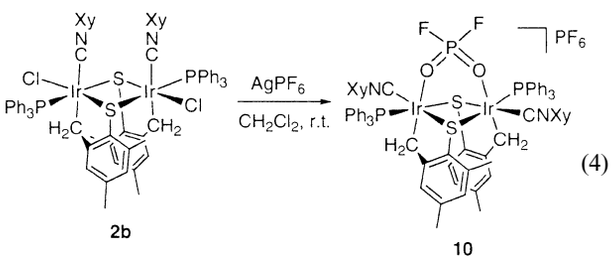

2b 10 (4)

a characteristic triplet ascribed to the bridging PF_2O_2 ligand; the ^1J(PF) value of 974 Hz is comparable to that observed in a related diruthenium complex, [{Ru(PFO$_3$)[P(OMe)$_3$]}$_2$(μ-S)-(μ-PF_2O_2)$_2$] (943 Hz).[21] The presence of the PF_2O_2 ligand is also suggested by the IR spectrum, which shows ν(PO) bands at 1142 and 1263 cm^{-1}, and a ν(PF) band at 841 cm^{-1}; a ν(NC) band due to the isocyanide ligands also appears at 2143 cm^{-1}. The molecular structure determined by an X-ray study is depicted in Fig. 9, and selected interatomic distances are listed

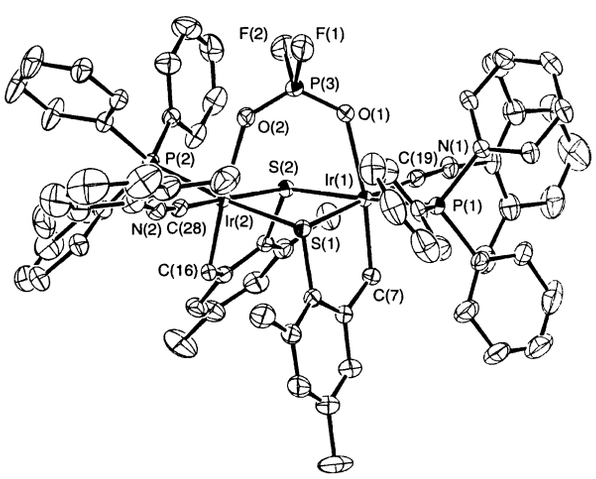

Fig. 9 Structure of the cationic part of **10**·CH_2Cl_2. All hydrogen atoms are omitted for clarity.

in Table 6. The bridging PF_2O_2 ligand is bound to the two Ir atoms through the O atoms. The Ir_2S_2 face is slightly puckered, with a dihedral angle of 17.1° around the S–S vector. The P–O [1.46 Å (mean)] and P–F distances [1.53 Å (mean)] are unexceptional compared to other difluorophosphato-bridged complexes.[21,22]

The transformation of the PF_6 anion into metal-bound PF_2O_2 is known to be mediated by transition metals, including iridium and silver.[21–23] The oxygen source in these reactions seems to be adventitious water rather than dioxygen. For example, Matsumoto *et al*. have reported that treatment of [{Ru(CH$_3$CN)$_3$[P(OMe)$_3$]$_2$}$_2$(μ-S_2)][PF_6]$_3$ with a mixture of acetylene and O_2 affords the PF_2O_2-bridged complex [{Ru-(PFO$_3$)[P(OMe)$_3$]$_2$}$_2$(μ-S)(μ-PF_2O_2)$_2$].[21] On the basis of a mass spectroscopic experiment using $^{18}O_2$, they have concluded that the oxygen atoms in the difluorophosphato ligand are derived from a trace amount of water in the solvent. On the other hand, $AgPF_6$ is hydrolyzed by trace amounts of water in dichloromethane, even in the absence of other transition metals.[23] Taking into account these examples, we believe that the oxygen atoms in complex **10** originate from adventitious water in the solvent or $AgPF_6$, although we have no information on which metals mediate the partial hydrolysis of the PF_6 anion, iridium, silver or both. We also carried out the reactions of **2** with AgOTf (OTf = OSO_2CF_3) and $AgBF_4$ instead of $AgPF_6$. However, the expected intermediates, such as coordinatively unsaturated cationic species, were not isolated from these reactions. Reactions of other dichloro complexes, such as **1**, **5** and **7**, with $AgPF_6$ also failed to give any characterizable products.

Concluding remarks

Our investigations into the reactivity of **1** have revealed that the diaryl disulfide ligand is easily replaced by a variety of substrates such as isocyanides, CO, hydrazines and hydroxylamine, as illustrated in Scheme 1. In other words, **1** has two adjacent coordination sites masked by the diaryl disulfide ligand. It should be noted that the dinuclear metallacycle structure remains intact in these substitution reactions, including the formation of the unprecedented dinuclear bis(hydroxylamine) complex **7**. In addition to the substitution reactions, hydrolysis of PF_6 anions takes place on treatment of the diiridium complex **2b** with $AgPF_6$. Reductive S–S bond cleavage of the disulfide complex **1b** provides an additional route for the generation of a coordinatively unsaturated bimetallic site on the thiairidacycles.

Experimental

General

All manipulations were carried out under an atmosphere of nitrogen by using standard Schlenk techniques. Solvents were dried by standard procedures and degassed before use. Isocyanides, hydrazines and aqueous hydroxylamine solution (50 wt%) were purchased and used as received. Complexes **1** were prepared as described previously.[3] ^{1}H (400 MHz) and ^{31}P-{^{1}H} (162 MHz) NMR spectra were recorded on a JEOL LA-400 spectrometer, whilst IR spectra were recorded on a Shimadzu 8100 spectrometer. Elemental analyses and FAB mass analysis were performed on a Perkin-Elmer 2400II CHN analyzer and a JEOL JM S600H spectrometer, respectively. The amounts of solvent molecules in the crystals were determined not only by elemental analyses, but also by ^{1}H NMR spectroscopic studies. ^{31}P {^{1}H} and ^{1}H NMR data for **2**–**10** are collected in Table 7.

Preparations

[Ir(μ-$SC_6H_2Me_2CH_2$)Cl(PPh$_3$)(XyNC)]$_2$ (2b). To an orange suspension of **1b** (260 mg, 0.164 mmol) in CH_2Cl_2 (20 cm^3) was added 2,6-xylyl isocyanide (47 mg, 0.358 mmol). The mixture was stirred at room temperature for 3 h, during which time the suspension gradually turned to a yellow solution. The solvent was removed under reduced pressure, and recrystallization of the resultant yellow solid from CH_2Cl_2 (3 cm^3)–MeOH (12 cm^3) afforded yellow crystals of **2b** (220 mg, 87%). $\tilde{\nu}_{max}$/cm^{-1} (KBr): 2126 (NC). Found: C, 55.68; H, 4.50; N, 1.78; $C_{72}H_{68}Cl_2Ir_2N_2P_2S_2$ requires C, 56.05; H, 4.44; N, 1.82%.

Table 7 ^{31}P-{^{1}H} and ^{1}H NMR spectroscopic data for complexes **2**–**10** (in $CDCl_3$, *J* in Hz)

		δ_H			
		Thiairidaindan			
Complex	δ_P (PPh_3)	$IrCH_2$	3,4,5-H[a]	4,6-Me[a]	Others
2a	−8.3	4.03 [2 H, d, ^{2}J(HH) 16.1]	6.75 (2 H, t, *J* 7.3)	2.16 (6 H, s)	7.5–7.0 (32 H, m, PPh_3 and 4-C_6H_2*H*Me_2NC)
		2.96 [2 H, dd, ^{2}J(HH) 16.1, ^{3}J(PH) 6.3]	6.65, 6.49 (2 H each, d, *J* 7.3)		6.86 (4 H, br d, 3,5-C_6*H*$_2$HMe_2NC, *J* 7.3)
					1.92 (12 H, br s, C_6H_3*Me*$_2$NC)
2b	−8.4	4.08 [2 H, d, ^{2}J(HH) 15.6]	6.35, 6.33 (2 H each, s)	2.19, 2.08 (6 H each, s)	7.4–6.8 (36 H, m, PPh_3 and C_6*H*$_3$$Me_2$NC),
		2.85 [2 H, dd, ^{2}J(HH) 15.6, ^{3}J(PH) 6.8]			1.89 (12 H, br s, C_6H_3*Me*$_2$NC)
3a	−8.0	3.93 [2 H, d, ^{2}J(HH) 15.6]	6.67 (2 H, t, *J* 7.3)	2.13 (6 H, s)	7.5–7.1 (30 H, m, PPh_3)
		2.75 [2 H, dd, ^{2}J(HH) 15.6, ^{3}J(PH) 6.8]	6.51, 6.45 (2 H each, d, *J* 7.3)		1.61 (18 H, s, Bu^{t}NC)
3b	−7.8	3.96 [2 H, d, ^{2}J(HH) 16.1]	6.34, 6.14 (2 H each, s)	2.14, 2.02 (6 H each, s)	7.5–7.1 (30 H, m, PPh_3)
		2.62 [2 H, dd, ^{2}J(HH) 15.9, ^{3}J(PH) 7.1]			1.58 (18 H, s, Bu^{t}NC)
4a	−7.4	3.78 [2 H, d, ^{2}J(HH) 16.5]	6.80 (2 H, t, *J* 7.4)	2.09 (6 H, s)	7.5–7.1 (30 H, m, PPh_3)
		2.91 [2 H, dd, ^{2}J(HH) 16.5, ^{3}J(PH) 8.9]	6.55 (4 H, d, *J* 7.6)		
4b	−7.2	3.83 [2 H, d, ^{2}J(HH) 16.1]	6.39, 6.30 (2 H each, s)	2.10, 2.08 (6 H each, s)	7.6–7.2 (30 H, m, PPh_3)
		2.80 [2 H, dd, ^{2}J(HH) 16.6, ^{3}J(PH) 8.3]			
5a[b]	−5.5	4.1 (2 H, m)	6.48, 6.21 (2 H each, d, *J* 7.3)	2.31 (6 H, s)	7.6–7.2 (30 H, m, PPh_3)
		3.68 [2 H, d, ^{2}J(HH) 15.6]	6.41 (2 H, t, *J* 7.3)		5.01, 4.55 [2 H each, br d, N_2H_4, ^{2}J(HH) 6.3]
5b[b]	−4.4	3.9 (2 H, m)	6.40, 6.02 (2 H each, s)	2.21, 1.97 (6 H each, s)	7.6–7.1 (30 H, m, PPh_3)
		3.54 [2 H, d, ^{2}J(HH) 15.7]			5.08, 4.67 [2 H each, br d, N_2H_4, ^{2}J(HH) 5.9]
6[b]	−7.7, −8.5 [1 P each, d, ^{4}J(PP) 15.1]	4.0–3.7 (3 H, m)	6.43 (1 H, d, *J* 7.3)	2.31, 2.14 (3 H each, s)	7.8–7.2 (30 H, m, PPh_3)
		3.32 [1 H, d, ^{2}J(HH) 16.1]	6.4–6.2 (3 H, m)		5.53, 4.66 [1 H each, d, NH_2, ^{2}J(HH) 10.7]
			6.05 (1 H, d, *J* 7.3)		2.74, 2.67 (3 H each, s, NMe_2)
			5.96 (1 H, d, *J* 7.8)		
7a	−7.2, −9.9 [1 P each, d, ^{4}J(PP) 15.3]	3.97 [1 H, dd, ^{2}J(HH) 16.6, ^{3}J(PH) 7.6]	6.6–6.0 (6 H, m)	2.37, 1.85 (3 H each, s)	10.08, 7.65, 6.22 (1 H each, NH_2OH)
		3.69 [1 H, d, ^{2}J(HH) 16.6]			7.76, 5.97, 5.84 (1 H each, NH_2OH)
		2.93 [1 H, d, ^{2}J(HH) 13.7]			7.6–7.1(30 H, m, PPh_3),
		2.73 [1 H, dd, ^{2}J(HH) 13.7, ^{3}J(PH) 7.1]			
7b	−6.7, −9.4 [1 P each, d, ^{4}J(PP) 15.3]	3.89 [1 H, dd, ^{2}J(HH) 15.6, ^{3}J(PH) 6.8]	6.38, 6.29, 6.09, 5.75 (1 H each, s)	2.33, 1.99, 1.79, 1.79 (3 H each, s)	9.97, 6.26 (1 H each, NH_2OH)
		3.78 [1 H, d, ^{2}J(HH) 15.6]			7.66, 5.92, 5.83 (1 H each, NH_2OH)
		3.04 [1 H, d, ^{2}J(HH) 13.7]			7.6–7.1 (31 H, m, PPh_3 and NH_2OH)
		2.51 [1 H, dd, ^{2}J(HH) 13.7, ^{3}J(PH) 7.1]			
8[c]	12.6	3.78 (2 H, br pseudo t)	5.98, 5.51 (2 H each, s)	2.26, 1.75, 1.32 (6 H each, s)[d]	8.4, 7.9 (4 H each, br s, PPh_3)
		3.62 (2 H, d, ^{2}J(HH) 12.2)			7.6 (6 H, br, PPh_3)
					7.5–7.3 (6 H, m, PPh_3)
					6.7 (2 H, br, PPh_3)
					6.5 (8 H, br, PPh_3)
					6.89, 6.33 (2 H each, s, SC_6*H*$_2$$Me_3$)
					2.43, 2.31 (6 H each, s, 2,6-SC_6H_2*Me*$_3$)
9[b,e]	−7.9	3.61 [2 H, d, ^{2}J(HH) 16.6]	6.38, 5.74 (2 H each, s)	2.41, 2.22, 1.88 (6 H each, s)[d]	7.3, 7.1 (30 H, br, PPh_3)
		2.6 (2 H, m)			6.98, 6.46 (2 H each, s, SC_6*H*$_2$$Me_3$)
					2.72, 1.54 (6 H each, s, 2,6-SC_6H_2*Me*$_3$)
10	164 [1 P, sept, ^{1}J(PF) 7.11][f]	3.41 [2 H, d, ^{2}J(HH) 14.1]	6.49, 6.04 (2 H each, s)	2.00, 1.81 (6 H each, s)	7.5–7.1 (36 H, m, PPh_3 and C_6*H*$_3$$Me_2$NC)
	4.4 (2 P, s)	2.80 [2 H, dd, ^{2}J(HH) 14.6, ^{3}J(PH) 7.3]			2.29 (12 H, s, C_6H_3*Me*$_2$NC)
	−10.1 [1 P, t, ^{1}J(PF) 974][g]				

[a] For a diagram showing the position numbers, see Fig. 2. [b] In CD_2Cl_2. [c] At −55 °C. [d] One of the three signals is attributed to 4-$SC_6H_2Me_2$*Me*. [e] At −50 °C. [f] Signal due to the PF_6 anion. [g] Signal due to the PF_2O_2 ligand.

[Ir(μ-SC$_6$H$_3$MeCH$_2$)Cl(PPh$_3$)(XyNC)]$_2$·0.5CH$_2$Cl$_2$ (2a·0.5CH$_2$Cl$_2$). This compound was prepared from **1a** by essentially the same procedure as that described for **2b**. Yield: 78%. $\tilde{\nu}_{max}$/cm^{-1} (KBr): 2128 (NC). Found: C, 53.95; H, 4.17; N, 1.74; $C_{70.5}H_{65}Cl_3Ir_2N_2P_2S_2$ requires C, 54.38; H, 4.21; N, 1.80%.

[Ir(μ-SC$_6$H$_3$MeCH$_2$)Cl(PPh$_3$)(Bu^{t}NC)]$_2$ (3a). This compound was prepared from **1a** and ^{t}BuNC by essentially the same procedure as that described for **2b**. Yield: 84%. $\tilde{\nu}_{max}$/cm^{-1} (KBr): 2145 (NC). Found: C, 52.30; H, 4.67; N, 1.94; $C_{62}H_{64}Cl_2Ir_2N_2P_2S_2$ requires C, 52.49; H, 4.55; N, 1.97%.

[Ir(μ-SC$_6$H$_2$Me$_2$CH$_2$)Cl(PPh$_3$)(Bu^{t}NC)]$_2$·0.5CH$_2$Cl$_2$ (3b·0.5CH$_2$Cl$_2$). This compound was prepared by essentially the same procedure as that described for **2b**, except using Bu^{t}NC instead of XyNC. Yield: 70%. $\tilde{\nu}_{max}$/cm^{-1} (KBr): 2147 (NC). Found: C, 51.79; H, 4.64; N, 1.80; $C_{64.5}H_{69}Cl_2Ir_2N_2P_2S_2$ requires C, 52.02; H, 4.67; N, 1.88%.

[Ir(μ-SC$_6$H$_3$MeCH$_2$)Cl(PPh$_3$)(CO)]$_2$·0.5C$_6$H$_5$CH$_3$ (4a·0.5C$_6$H$_5$CH$_3$). A CH_2Cl_2 (5 cm^3) suspension of **1a**·2CH_2Cl_2 (72 mg, 0.424 mmol) was stirred at room temperature under CO for 1 h. After the solvent was removed under reduced pressure, the residue was dissolved in CH_2Cl_2 and chromatographed on alumina. The yellow band eluted with CH_2Cl_2–hexane (2 : 1) was collected and recrystallized from toluene (1.5 cm^3)–MeOH (9 cm^3), giving yellow crystals of **4a**·0.5$C_6H_5CH_3$ (48 mg, 84%). $\tilde{\nu}_{max}$/cm^{-1} (KBr): 2047(sh), 2039 (CO). Found: C, 50.80; H, 3.75; $C_{57.5}H_{50}Cl_2Ir_2O_2P_2S_2$ requires C, 50.99; H, 3.72%.

[Ir(μ-SC$_6$H$_2$Me$_2$CH$_2$)Cl(PPh$_3$)(CO)]$_2$ (4b). This compound was prepared from **1b** by essentially the same procedure as that described for **4a**. Yield: 73%. $\tilde{\nu}_{max}$/cm^{-1} (KBr): 2043, 2022(sh) (CO). Found: C, 50.87; H, 3.84; $C_{56}H_{50}Cl_2Ir_2O_2P_2S_2$ requires C, 50.33; H, 3.77%.

[{Ir(μ-SC$_6$H$_3$MeCH$_2$)Cl(PPh$_3$)}$_2$(μ-NH$_2$NH$_2$)] (5a). To an orange suspension of **1a**·2CH_2Cl_2 (403 mg, 0.238 mmol) in CH_2Cl_2 (20 cm^3) was added anhydrous hydrazine (0.010 cm^3, 0.30 mmol). The mixture was stirred for 2 h at room temperature and then evaporated *in vacuo*. Recrystallization of the yellow residue from CH_2Cl_2 (11 cm^3)–MeOH (40 cm^3) afforded **5a** as a yellow solid (309 mg, 91%). $\tilde{\nu}_{max}$/cm^{-1} (KBr): 3295, 3270, 3229, 3141 (NH). Found: C, 48.77; H, 4.03; N, 2.19; $C_{52}H_{50}Cl_2Ir_2N_2P_2S_2$ requires C, 48.63; H, 3.92; N, 2.18%. The single crystal used in the X-ray diffraction study was obtained by recrystallization from $CHCl_3$–Pr^{i}OH.

[{Ir(μ-SC$_6$H$_2$Me$_2$CH$_2$)Cl(PPh$_3$)}$_2$(μ-NH$_2$NH$_2$)] (5b). This compound was prepared from **1b** by essentially the same procedure as that described for **5a**. Yield: 55%. $\tilde{\nu}_{max}$/cm^{-1} (KBr): 3229, 3301 (NH). Found: C, 48.89; H, 4.13; N, 2.23; $C_{54}H_{54}Cl_2Ir_2N_2P_2S_2$ requires C, 49.42; H, 4.15; N, 2.13%.

[{Ir(μ-SC$_6$H$_3$MeCH$_2$)Cl(PPh$_3$)}$_2$(μ-NH$_2$NMe$_2$)]·0.5CH$_2$Cl$_2$ (6·0.5CH$_2$Cl$_2$). This compound was prepared by essentially the same procedure as that described for **5a**, except using NH_2NMe_2 instead of N_2H_4. Yield: 88%. $\tilde{\nu}_{max}$/cm^{-1} (KBr): 3262, 3189 (NH). Found: C, 48.19; H, 4.10; N, 2.05; $C_{54.5}H_{55}Cl_3Ir_2N_2P_2S_2$ requires C, 48.31; H, 4.09; N, 2.07%. The single crystal used in the X-ray diffraction study was obtained by recrystallization from CH_2Cl_2–MeOH.

[Ir(μ-SC$_6$H$_3$MeCH$_2$)Cl(PPh$_3$)(NH$_2$OH)]$_2$ (7a). To an orange solution of **1a**·2CH_2Cl_2 (86 mg, 0.0506 mmol) in CH_2Cl_2 (10 cm^3) was added aqueous hydroxylamine (0.007 cm^3, 0.11 mmol), and the mixture was stirred at room temperature for 2 h. The resultant yellow solution was evaporated to dryness *in vacuo*, and the residue was recrystallized from CH_2Cl_2 (2.5 cm^3)–Et_2O (10 cm^3). Yellow crystals of **7a**·Et_2O were collected by filtration and subjected to an X-ray analysis. The thoroughly dried sample was found to lose the solvating ether molecule on the basis of ^{1}H NMR spectroscopy and combustion analysis. Yield: 60 mg (90%). $\tilde{\nu}_{max}$/cm^{-1} (KBr): 3279(sh), 3270, 3231, 3202, 3129, 3110(sh) (NH and OH). Found: C, 47.66; H, 4.28; N, 2.00; $C_{52}H_{52}Cl_2Ir_2N_2O_2P_2S_2$ requires C, 47.37; H, 3.98; N, 2.12%.

[Ir(μ-SC$_6$H$_2$Me$_2$CH$_2$)Cl(PPh$_3$)(NH$_2$OH)]$_2$·0.5CH$_2$Cl$_2$ (7b·0.5CH$_2$Cl$_2$). This compound was prepared from **1b** by essentially the same procedure as that described for **7a**. Yield: 64%. $\tilde{\nu}_{max}$/cm^{-1} (KBr): 3274, 3204, 3133, 3112(sh) (NH and OH). Found: C, 47.55; H, 4.37; N, 2.19; $C_{54.5}H_{57}Cl_3Ir_2N_2O_2P_2S_2$ requires C, 47.13; H, 4.14; N, 2.02%.

[Ir(μ-SC$_6$H$_2$Me$_2$CH$_2$)(SMes)(PPh$_3$)]$_2$·0.5CH$_2$Cl$_2$ (8·0.5CH$_2$Cl$_2$). To a suspension of **1b** (100 mg, 0.0632 mmol) in THF (10 cm^3) was added a 1.02 M solution of MeLi in Et_2O (0.13 cm^3, 0.132 mmol), and the mixture was stirred at room temperature. Within 1 h, the orange suspension gradually turned to a dark green solution, which was then evaporated to dryness *in vacuo*. The resultant green solid was washed with MeOH (3 cm^3). Subsequent recrystallization from CH_2Cl_2 (2 cm^3)–Pr^{i}OH (10 cm^3) afforded black crystals of **8**·0.5CH_2Cl_2 (31 mg, 32%). Found: C, 56.15; H, 4.75; $C_{72.5}H_{73}ClIr_2P_2S_4$ requires C, 56.02; H, 4.73%.

[Ir(μ-SC$_6$H$_2$Me$_2$CH$_2$)(SMes)(PPh$_3$)(CO)]$_2$ (9). A dark green solution of **8**·0.5CH_2Cl_2 (55 mg, 0.0354 mmol) in CH_2Cl_2 (5 cm^3) was exposed to CO gas (1 atm), and the solution was stirred at room temperature for 15 min. The resultant orange solution was evaporated, and the residue was recrystallized from CH_2Cl_2 (2 cm^3)–Pr^{i}OH (10 cm^3). The orange crystals of **9**·2CH_2Cl_2 that formed were collected by filtration and subjected to X-ray analysis. The thoroughly dried sample was found to lose the solvating CH_2Cl_2 molecule on the basis of ^{1}H NMR spectroscopy and combustion analysis. Yield: 41 mg, 74%. $\tilde{\nu}_{max}$/cm^{-1} (KBr): 2035 (CO). Found: C, 56.61; H, 4.58; $C_{74}H_{72}Ir_2O_2P_2S_2$ requires C, 56.68; H, 4.63%.

[{Ir(μ-SC$_6$H$_2$Me$_2$CH$_2$)(PPh$_3$)(XyNC)}$_2$(μ-PF$_2$O$_2$)][PF$_6$] (10). To a CH_2Cl_2 solution (7 cm^3) of **2b** (59 mg, 0.0382 mmol) was added $AgPF_6$ (20 mg, 0.0791 mmol), and the mixture was stirred at room temperature for 1 h. After filtering off the white precipitate that formed, the pale yellow filtrate was evaporated to dryness. Recrystallization of the pale yellow residual solid from CH_2Cl_2 (2.5 cm^3)–Et_2O (10 cm^3) gave pale yellow crystals of **10**·CH_2Cl_2, which were collected by filtration and subjected to X-ray analysis. The thoroughly dried sample was found to contain no solvating CH_2Cl_2 molecule on the basis of ^{1}H NMR spectroscopy and combustion analysis. Yield: 43 mg, 66%. $\tilde{\nu}_{max}$/cm^{-1} (KBr): 2143 (NC), 1263 and 1142 (PO), 841 (PF). FAB MS *m/z*: 1573 [{Ir(μ-SC$_6$H$_2$Me$_2$CH$_2$)(PPh$_3$)(XyNC)}$_2$(μ-PF$_2$O$_2$)]$^+$. Found: C, 50.36; H, 4.10; N, 1.54; $C_{72}H_{68}F_8Ir_2N_2O_2P_4S_2$ requires C, 50.34; H, 3.99; N, 1.63%.

Crystallography

Diffraction data were collected on a Rigaku AFC7R four-circle automated diffractometer with graphite-monochromatized Mo-Kα radiation (λ = 0.71069 Å). The data collections were performed at room temperature using the ω (for **5a**·Pr^{i}OH, **6**·0.5CH_2Cl_2, **9**·2CH_2Cl_2 and **10**·CH_2Cl_2) or ω–2θ (for **2b**, **4a**·0.5$C_6H_5CH_3$, **7a**·Et_2O and **8**·0.5CH_2Cl_2) scan techniques at a rate of 32° min^{-1}, to maximum 2θ values of 50° (for **6**·0.5CH_2Cl_2 and **9**·2CH_2Cl_2) and 55° (all others). The

Table 8 Crystal data for **2b**, **4a**·0.5$C_6H_5CH_3$, **5a**·Pr^iOH, **7a**·Et_2O, **8**·0.5CH_2Cl_2, **9**·2CH_2Cl_2 and **10**·CH_2Cl_2

	2b	**4a**·0.5$C_6H_5CH_3$	**5a**·Pr^iOH	**7a**·Et_2O	**8**·0.5CH_2Cl_2	**9**·2CH_2Cl_2	**10**·CH_2Cl_2
Formula	$C_{72}H_{68}Cl_2Ir_2N_2P_2S_2$	$C_{57.5}H_{50}Cl_2Ir_2O_2P_2S_2$	$C_{55}H_{58}Cl_2Ir_2N_2OP_2S_2$	$C_{56}H_{62}Cl_2Ir_2N_2O_3P_2S_2$	$C_{72.5}H_{73}ClIr_2P_2S_4$	$C_{76}H_{76}Cl_4Ir_2O_2P_2S_4$	$C_{73}H_{70}Cl_2F_8Ir_2N_2O_2P_2S_2$
M	1542.76	1354.44	1344.49	1392.53	1554.45	1737.87	1802.72
Crystal system	Monoclinic	Monoclinic	Monoclinic	Triclinic	Triclinic	Triclinic	Monoclinic
Space group	*C*2/*c* (no. 15)	*P*2/*n* (no. 13)	*P*2$_1$/*n* (no. 14)	*P*$\bar{1}$ (no. 2)	*P*$\bar{1}$ (no. 2)	*P*$\bar{1}$ (no. 2)	*P*2$_1$/*a* (no. 14)
a/Å	21.610(2)	23.234(3)	13.809(10)	11.606(5)	11.150(3)	11.212(4)	14.066(3)
b/Å	14.329(8)	10.403(2)	11.39(1)	11.975(6)	14.140(2)	15.345(4)	31.964(4)
c/Å	22.434(2)	23.726(3)	32.825(8)	19.977(7)	22.018(5)	24.013(6)	16.355(2)
α/°	90	90	90	88.04(4)	82.95(2)	105.97(2)	90
β/°	113.610(7)	109.76(1)	97.83(4)	87.40(3)	79.64(2)	93.84(3)	91.83(1)
γ/°	90	90	90	74.64(4)	79.26(2)	109.26(2)	90
U/Å^3	6365(3)	5396(1)	5115(5)	2673(1)	3340(1)	3692(2)	7287(1)
Z	4	4	4	2	2	2	4
μ(Mo-K*α*)/cm^{-1}	44.32	52.17	55.02	52.69	42.40	39.55	39.43
D_c/g cm^{-3}	1.610	1.667	1.746	1.730	1.545	1.563	1.643
No. unique reflections	7310	12 393	11 736	12 288	15 375	13 002	16 771
R_{int}	0.019	0.038	0.034	0.017	0.060	0.023	0.028
No. data used [$I > 3\sigma(I)$]	4900	7225	8302	9653	9486	8483	10 801
No. variables	371	578	595	623	721	806	851
R; R_w [a]	0.034; 0.035	0.041; 0.046	0.035; 0.039	0.033; 0.039	0.045; 0.050	0.043; 0.049	0.039; 0.038

[a] $R = \Sigma||F_o| - |F_c||/\Sigma|F_o|$; $R_w = [\Sigma w(|F_o| - |F_c|)^2/\Sigma wF_o^2]^{1/2}$; $w = 1/\sigma^2(F_o)$.

intensities of three standard reflections were monitored every 150 reflections during the data collection, showing no significant decay for **2b**, **4a**·0.5$C_6H_5CH_3$, **5a**·Pr^iOH, **8**·0.5CH_2Cl_2 and **10**·CH_2Cl_2, but steady decreases in intensity were observed for **7a**·Et_2O (21.4%) and **9**·2CH_2Cl_2 (5.5%), to which corrections for the decay were applied. Details of the crystals and data collection parameters are summarized in Table 8.

The structure solutions and refinements were carried out by using the TEXSAN crystallographic software package.[24] The positions of the non-hydrogen atoms were determined by Patterson methods (DIRDIF PATTY[25]) and subsequent Fourier syntheses. All non-hydrogen atoms were refined by full-matrix least-squares techniques (based on *F*) with anisotropic thermal parameters for **2b**, **5a**·Pr^iOH, **7a**·Et_2O and **10**·CH_2Cl_2. For **4a**·0.5$C_6H_5CH_3$, the solvating toluene molecule was placed at two disordered positions and the corresponding carbon atoms were included in the refinement with fixed parameters with a 50% occupancy. For **8**·0.5CH_2Cl_2, the carbon and chlorine atoms in the solvating molecule were included in the refinement with fixed parameters, whilst the carbon atom [C(77)] of one of the solvating molecules in **9**·2CH_2Cl_2 was refined with isotropic parameters. The hydroxy hydrogen atom of **5a**·Pr^iOH and the hydrogen atoms of the solvating molecules in **4a**·0.5$C_6H_5CH_3$ and **8**·0.5CH_2Cl_2 were not located. One of the hydroxy hydrogen atoms in **7a**·Et_2O was found in the difference Fourier map and included in the refinement with fixed parameters, while the other was not located. All the other hydrogen atoms were placed at calculated positions (d_{C-H} = 0.95 Å) and included in the final stages of the refinements with fixed parameters.

For **6**·0.5CH_2Cl_2, the refinement has not been completed because large residual electron densities in the difference Fourier map could not be dealt with properly. Crystal data: triclinic; space group *P*$\bar{1}$ (no. 2), *a* = 14.898(4), *b* = 15.029(3), *c* = 26.191(10) Å, *α* = 99.11(2), *β* = 92.41(3), *γ* = 90.59(2)°, *U* = 5784(2) Å^3, *Z* = 4; no. of unique reflections, 24 214. In the refinement, all atoms, except for those in the solvating molecule, were treated as in the other complexes. The chlorine and carbon atoms in the solvating CH_2Cl_2 molecule were refined isotropically. The refinement was also hampered by a significant decay of the reflections during the data collection (average 30.3% decrease for the three reference reflections at the final stage). The distances and angles described in the text are based on the stage of the refinement with the *R* (R_w) values of 0.064 (0.085) for $I > 3\sigma(I)$ and the gof value of 2.16.

CCDC reference numbers 179459–179465.

See http://www.rsc.org/suppdata/dt/b2/b201591a/ for crystallographic data in CIF or other electronic format.

Acknowledgements

This work was supported by the Ministry of Education, Culture, Sports, Science and Technology of Japan and the JSPS FY2000 "Research for the Future Program".

References

1 *Catalysis by Di- and Polynuclear Metal Cluster Complexes*, ed. R. D. Adams and F. A. Cotton, Wiley-VCH, New York, 1998.
2 S. Matsukawa, S. Kuwata and M. Hidai, *Inorg. Chem. Commun.*, 1998, **1**, 368.
3 S. Matsukawa, S. Kuwata and M. Hidai, *Inorg. Chem.*, 2000, **39**, 791.
4 D. Carrillo, *Coord. Chem. Rev.*, 1992, **119**, 137; R. D. Adams, *Acc. Chem. Res.*, 2000, **33**, 171; N. Kuhn and H. Schumann, *J. Organomet. Chem.*, 1985, **287**, 345; A. Shaver, M. El-khateeb and A.-M. Lebuis, *Inorg. Chem.*, 1995, **34**, 3841.
5 M. Hidai, Y. Mizobe and H. Matsuzaka, *J. Organomet. Chem.*, 1994, **473**, 1; M. Hidai and Y. Mizobe, in *Transition Metal Sulfur Chemistry: Biological and Industrial Significance*, ed. E. I. Stiefel and K. Matsumoto, American Chemical Society, Washington, DC, 1996, p. 310; Y. Ishii, K. Ogio, M. Nishio, M. Retbøll, S. Kuwata, H. Matsuzaka and M. Hidai, *J. Organomet. Chem.*, 2000, **599**, 221;

Y. Nishibayashi, I. Wakiji and M. Hidai, *J. Am. Chem. Soc.*, 2000, **122**, 11019; Y. Nishibayashi, I. Wakiji, Y. Ishii, S. Uemura and M. Hidai, *J. Am. Chem. Soc.*, 2001, **123**, 3393; Y. Nishibayashi, M. Yamanashi, I. Wakiji and M. Hidai, *Angew. Chem., Int. Ed.*, 2000, **39**, 2909.
6 B. K. Burgess and D. J. Lowe, *Chem. Rev.*, 1996, **96**, 2983.
7 L. Vaska and J. W. DiLuzio, *J. Am. Chem. Soc.*, 1962, **84**, 679.
8 J. W. Kang and P. M. Maitlis, *J. Organomet. Chem.*, 1971, **26**, 393.
9 B. T. Heaton, C. Jacob and P. Page, *Coord. Chem. Rev.*, 1996, **154**, 193.
10 F. Y. Pétillon, P. Schollhammer, J. Talarmin and K. W. Muir, *Coord. Chem. Rev.*, 1998, **178–180**, 203; P. Schollhammer, E. Guénin, F. Y. Pétillon, J. Talarmin, K. W. Muir and D. S. Yufit, *Organometallics*, 1998, **17**, 1922; F. Y. Pétillon, P. Schollhammer, J. Talarmin and K. W. Muir, *Inorg. Chem.*, 1999, **38**, 1954; D. Coucouvanis, P. E. Mosier, K. D. Demadis, S. Patton, S. M. Malinak, C. G. Kim and M. A. Tyson, *J. Am. Chem. Soc.*, 1993, **115**, 12193; P. E. Mosier, C. G. Kim and D. Coucouvanis, *Inorg. Chem.*, 1993, **32**, 2620; M. Herberhold, H. Yan and W. Milius, *J. Organomet. Chem.*, 2000, **598**, 142; K. Mashima, S. Kaneko, K. Tani, H. Kaneyoshi and A. Nakamura, *J. Organomet. Chem.*, 1997, **545–546**, 345; M. Kawano, C. Hoshino and K. Matsumoto, *Inorg. Chem.*, 1992, **31**, 5158; K. Matsumoto, H. Uemura and M. Kawano, *Chem. Lett.*, 1994, 1215; T. Funahashi, M. Kawano, Y. Koide, R. Somazawa and K. Matsumoto, *Inorg. Chem.*, 1999, **38**, 109; K. Matsumoto, T. Koyama and Y. Koide, *J. Am. Chem. Soc.*, 1999, **121**, 10913; D. Shaowu, Z. Nianyong and L. Jiaxi, *Inorg. Chem.*, 1992, **31**, 2847.
11 S. Kuwata, Y. Mizobe and M. Hidai, *Inorg. Chem.*, 1994, **33**, 3619.
12 T. Masumori, H. Seino, Y. Mizobe and M. Hidai, *Inorg. Chem.*, 2000, **39**, 5002.
13 H. D. Flack and E. Parthé, *Acta Crystallogr., Sect. B*, 1973, **29**, 1099; A. J. Deeming, S. Doherty, J. E. Marshall, J. L. Powell and A. M. Senior, *J. Chem. Soc., Dalton Trans.*, 1993, 1093; E. Garnier and M. Bele, *Acta Crystallogr., Sect. C*, 1993, **49**, 2066; E. Bernhardt and W. Preetz, *Z. Anorg. Allg. Chem.*, 1997, **623**, 1389; V. M. Deflon, C. M. Mössmer and J. Strähle, *Z. Anorg. Allg. Chem.*, 1999, **625**, 2186.
14 G. Albertin, S. Antoniutti, E. Bordignon and F. Menegazzo, *J. Chem. Soc., Dalton Trans.*, 2000, 1181; J.-T. Chen, Y.-K. Chen, J.-B. Chu, G.-H. Lee and Y. Wang, *Organometallics*, 1997, **16**, 1476; W. Xu, A. J. Lough and R. H. Morris, *Inorg. Chem.*, 1996, **35**, 1549.
15 T. V. Ashworth, M. J. Nolte, R. H. Reimann and E. Singleton, *J. Chem. Soc., Chem. Commun.*, 1977, 757; T. V. Ashworth, M. J. Nolte, R. H. Reimann and E. Singleton, *J. Chem. Soc., Dalton Trans.*, 1988, 1043.
16 J. A. McCleverty, *Transition Met. Chem.*, 1987, **12**, 282.
17 B. A. Averill, *Chem. Rev.*, 1996, **96**, 2951.
18 J. N. Younathan, K. S. Wood and T. J. Meyer, *Inorg. Chem.*, 1992, **31**, 3280.
19 (*a*) J. S. Southern, G. L. Hillhouse and A. L. Rheingold, *J. Am. Chem. Soc.*, 1997, **119**, 12406; T. Y. Cheng, A. Ponce, A. L. Rheingold and G. L. Hillhouse, *Angew. Chem., Int. Ed. Engl.*, 1994, **33**, 657; (*b*) L. M. Engelhardt, P. W. G. Newman, C. L. Raston and A. H. White, *Aust. J. Chem.*, 1974, **27**, 503.
20 Y. Nishibayashi, M. Yamanashi, Y. Takagi and M. Hidai, *Chem. Commun.*, 1997, 859; Y. Takagi, H. Matsuzaka, Y. Ishii and M. Hidai, *Organometallics*, 1997, **16**, 4445 and references therein.
21 K. Matsumoto, Y. Sano, M. Kawano, H. Uemura, J. Matsunami and T. Sato, *Bull. Chem. Soc. Jpn.*, 1997, **70**, 1239.
22 S. J. Thompson, P. M. Bailey, C. White and P. M. Maitlis, *Angew. Chem., Int. Ed. Engl.*, 1976, **15**, 490; C. White, S. J. Thompson and P. M. Maitlis, *J. Organomet. Chem.*, 1977, **134**, 319; L. Chen, M. A. Khan and G. B. Richter-Addo, *Inorg. Chem.*, 1998, **37**, 533; S. Kitagawa, M. Kondo, S. Kawata, S. Wada, M. Maekawa and M. Munakata, *Inorg. Chem.*, 1995, **34**, 1455 and references therein.
23 R. Fernández-Galán, B. R. Manzano, A. Otero, M. Lanfranchi and M. A. Pellinghelli, *Inorg. Chem.*, 1994, **33**, 3209.
24 TEXSAN, Crystal Structure Analysis Package, Molecular Structure Corp., The Woodlands, TX, USA, 1985 and 1999.
25 P. T. Beurskens, G. Admiraal, G. Beurskens, W. P. Bosman, R. de Gelder, R. Israel and J. M. M. Smits, The DIRDIF-94 Program System, Technical Report of the Crystallography Laboratory, University of Nijmegen, The Netherlands, 1994.